Applied Catalysis B: Environmental 156–157 (2014) 53–61

Contents lists available at ScienceDirect

Applied Catalysis B: Environmental

journal homepage: www.elsevier.com/locate/apcatb

ZrO_2-modified Al_2O_3-supported PdCu catalysts for the water denitrification reaction

María A. Jaworski[a], Ileana D. Lick[a], Guillermo J. Siri[a,b], Mónica L. Casella[a,*]

[a] CINDECA (CCT La Plata-CONICET, UNLP), Universidad Nacional de La Plata, Facultad de Ciencias Exactas, 47 N°257, 1900 La Plata, Argentina
[b] PIDCAT Facultad de Ingeniería, Universidad Nacional de La Plata, 1 y 47, 1900 La Plata, Argentina

ARTICLE INFO

Article history:
Received 6 November 2013
Received in revised form 14 January 2014
Accepted 28 February 2014
Available online 12 March 2014

Keywords:
Nitrate
Nitrite
Water denitrification
PdCu catalysts
Zirconia

ABSTRACT

Monometallic Pd and bimetallic Pd–Cu catalysts supported on alumina, zirconia and ZrO_2–Al_2O_3 mixed oxides of different composition were prepared and evaluated in the catalytic denitrification of water. The supports were characterized by X-ray diffraction (XRD), scanning electron microscopy with energy dispersive X-ray (SEM/EDX), NH_3-adsorption thermogravimetry and specific surface areas measured by the BET method. XRD studies showed that the predominant phase in the ZrO_2-modified Al_2O_3 supports is the metastable tetragonal phase (57%) of zirconia. SEM/EDX results indicated that ZrO_2 crystals are distributed homogeneously on the supports. Temperature-programmed reduction (TPR) experiments carried out on bimetallic PdCu catalysts showed that Pd is well dispersed on the modified supports and that there is a strong interaction between both metals. The modification of Al_2O_3 by the addition of ZrO_2 not only improved the activity but also the selectivity to N_2 of the PdCu catalysts.

© 2014 Elsevier B.V. All rights reserved.

1. Introduction

Nowadays, groundwater used for human consumption is contaminated with NO_3^- concentrations well above the maximum level allowed by the U.S. Environmental Protection Agency (10 ppm) [1]. Nitrate excess in water is mainly caused by fertilizers and waste effluents from certain industries.

The consumption of water with excess NO_3^- seriously affects human health mainly because it is reduced to NO_2^- in the human body. NO_2^- is combined with hemoglobin, which favors methemoglobinemia especially in children under six months who may suffer from the so-called "blue baby syndrome" that in many cases leads to death [2]. Moreover, NO_2^- could be converted into carcinogenic nitrosamine.

The reduction and elimination of NO_3^- from aqueous solutions using hydrogen over a solid catalyst is one of the most promising technologies. Most catalysts for nitrate reduction are composed of a noble metal and a promoter. The great majority of the bimetallic catalytic systems used in the denitrification of water are composed of noble metals such as Pd, Pt, Ru, Rh, or Ir and promoted by Cu, Sn, Ag, or In [3–5].

It is well-known that the performance of catalysts depends on the nature and structure of the active phase and the chemical and textural characteristics of the support. Different solids have been employed as supports in catalysts for the denitrification of water: alumina [6–8], zirconia, titania [9,10], activated carbon [11,12], SnO_2 [13], ceria [14], SiO_2 [15] and Mg/Al layered double hydroxide [16], and it has been demonstrated that different supports significantly affect the catalytic activity and selectivity of the process. Recently, Soares et al. reported a very complete study in which they used different materials as support, showing the remarkable effect they had on the performance of PdCu catalysts [17].

In the case of inert supports such as SiO_2 or Al_2O_3, one of the most widely accepted mechanisms for the reduction of NO_3^- involves its reduction to intermediate nitrite or directly to nitrogen gas or ammonium ion [6,18]. Since Vorlop et al. [19] published in 1989 the first study using solid catalysts for the removal of NO_3^- to date, bimetallic PdCu systems have been the most successful in terms of activity. According to the most accepted explanation, in these catalysts, bimetallic sites allow the reduction of NO_3^- to NO_2^-, which is then reduced to N_2 or over-reduced to NH_4^+ on monometallic Pd sites [20,21].

Zirconia has been used as support for catalysts and has received considerable attention due to a special combination of surface properties. It possesses chemical properties that may be of importance in the behavior of catalytic systems, namely acidity or basicity, as well as in their reducing and oxidizing ability [22,23].

* Corresponding author. Tel.: +54 2214210711.
E-mail addresses: casella@quimica.unlp.edu.ar, monicalauracasella30@gmail.com (M.L. Casella).

http://dx.doi.org/10.1016/j.apcatb.2014.02.048
0926-3373/© 2014 Elsevier B.V. All rights reserved.

Table 1
Nomenclature, textural properties and acidity of the prepared supports.

Nomenclature	Composition	S_{BET} ($m^2\ g^{-1}$)	V_p ($cm^3\ g^{-1}$)[b]	D_p (nm)[a]	Acidity (μmol $NH_3\ m^{-2}$)
Z_f	ZrO_2 (as prepared)	309	0.18	2.4	n.d.
Z	ZrO_2 (calcined at 600 °C)	73	0.10	5.4	0.80
A	Al_2O_3 (calcined at 600 °C)	190	0.47	10.1	1.47
ZA-5	5 wt.%ZrO_2/Al_2O_3	184	0.47	10.2	1.47
ZA-10	10 wt.%ZrO_2/Al_2O_3	179	0.44	10.1	2.18
ZA-15	15 wt.%ZrO_2/Al_2O_3	175	0.46	9.9	3.40

[a] D_p (pore diameter) was estimated from BJH desorption determination.
[b] V_p (pore volume) was estimated from the pore volume determined using the adsorption branch of the nitrogen isotherm curve at $P/P_0 = 0.98$ single point.

With Pd as the active phase, ZrO_2 has been used in various oxidation reactions, such as the oxidation of CH_4 [24] and toluene [25]. In the case of a reduction reaction such as water denitrification, the use of zirconia as a slightly conventional support is interesting to study because of its capability to improve the performance of supported transition metals in hydrogenation reactions.

Despite its beneficial influence on the catalytic activity, the zirconia support has a low surface area. For that reason, this solid is often deposited on high surface area oxides, such as alumina or silica, in order to prepare ZrO_2 supports with greater area [26–28]. Zirconium oxide dispersed on alumina and silica is an attractive new class of supports, combining the unique chemical properties of ZrO_2 with the high surface area and the mechanical stability of alumina or silica supports [29]. It is possible to adjust the textural properties of ZrO_2–Al_2O_3 mixed oxides by changing the ratio of the two oxides during the preparation procedure to thereby design catalysts that are more selective [22].

The objectives of the present study were to develop monometallic Pd and bimetallic Pd–Cu catalysts supported on different oxides and to evaluate their activity and selectivity toward the catalytic denitrification of water. Alumina, zirconia and ZrO_2–Al_2O_3 mixed oxides of different composition were used as supports, employing a sol–gel procedure to prepare the ZrO_2-containing solids. These supports were characterized by X-ray diffraction (XRD), scanning electron microscopy with energy dispersive X-ray (SEM/EDX), NH_3-adsorption thermogravimetry and specific surface areas measured by the BET method. Besides, the reducibility of the mono- and bimetallic catalysts was studied by temperature-programmed reduction (TPR) experiments.

2. Experimental

2.1. Support preparation

2.1.1. ZrO_2 preparation

The precursor salt, $ZrOCl_2{\cdot}8H_2O$ (Fluka), was dissolved in distilled water. Aqueous ammonia was added until the pH of the solution reached a value of 10 and the formation of the gel was observed. The mixture was aged for 8 days at room temperature. The obtained precipitate was washed with distilled water until free from chloride ions (determined by $AgNO_3$), filtered and dried at 105 °C for 24 h. The hydrous zirconia was calcined at 600 °C for 2 h. The following equation represents the zirconia preparation:

$$ZrOCl_2{\cdot}6H_2O + OH^- \rightarrow ZrO_2 + 2Cl^- + H^+ + 6H_2O$$

2.1.2. ZrO_2–Al_2O_3 preparation

Zirconia particles were grown onto the γ-Al_2O_3 support (Air Products, surface area 190 $m^2\ g^{-1}$; pore volume 0.50 $m^3\ g^{-1}$) by adding a $ZrOCl_2{\cdot}6H_2O$ solution onto γ-Al_2O_3 in an appropriate concentration so as to obtain 5, 10 and 15 wt.% ZrO_2 on Al_2O_3. In a typical procedure, the alumina support was suspended in deionized water under vigorous stirring. The appropriate amount of $ZrOCl_2{\cdot}6H_2O$ was dissolved into the resultant mixture and aqueous ammonia was added dropwise until pH = 10. After aging the solids for 8 days, they were washed until no chloride ion could be detected with $AgNO_3$ solution in the filtrate. The materials obtained were dried at 105 °C and finally calcined at 600 °C for 2 h. These supports are designated ZA-*x*, where "*x*" indicates the ZrO_2 content.

Both the as-received commercial γ-Al_2O_3 and the γ-Al_2O_3 calcined at 600 °C (A) for 2 h were used for comparison purposes. The nomenclature of the supports is described in Table 1.

2.2. Catalyst preparation

The monometallic catalysts were prepared by impregnation using an aqueous solution of H_2PdCl_4 prepared from $PdCl_2$ (Sigma–Aldrich) in HCl (pH = 1) in order to obtain a catalyst containing 1 wt.% of palladium. The support was suspended in the aqueous solution containing the palladium salt for 24 h at room temperature. Then, the solids were dried at 105 °C and calcined at 400 °C for 2 h. To prepare the bimetallic catalysts, a certain amount of the monometallic catalyst was added to a solution of copper nitrate ($Cu(NO_3)_2$, Merck) of the appropriate concentration. This mixture was stirred for 2 h before drying at 105 °C and calcined at 400 °C (2 h). The catalysts are designated Pd/support or PdCu/support (see Table 2).

2.3. Characterization of supports and catalysts

The textural properties of the supports (specific surface area, S_{BET}, and pore volume) were measured by N_2 adsorption–desorption at −196 °C using a Micromeritics Accusorb 2100E apparatus. The S_{BET} was calculated by the BET equation and the pore volume (V_p) was estimated using the adsorption branch of the nitrogen isotherm curve at $P/P_0 = 0.98$ single point. The textural properties of the supports are listed in Table 1.

The structural characterization was completed by X-ray powder diffraction (XRD) performed on a Philips PW 1050/70 diffractometer using Cu Kα radiation ($\lambda = 0.154$ nm). XRD data were recorded in the range of $2\theta = 5°$–$70°$ at a scanning speed of 2° min^{-1}. The

Table 2
Nomenclature and chemical composition of Pd and PdCu studied catalysts.

Nomenclature	Pd (wt.%)	Cu (wt.%)	Support
Pd/γ-Al_2O_3	1.0	–	Commercialγ-Al_2O_3
PdCu0.5/γ-Al_2O_3	1.0	0.3	Commercialγ-Al_2O_3
PdCu1/γ-Al_2O_3	1.0	0.6	Commercialγ-Al_2O_3
Pd/A	1.0	–	Al_2O_3 (calcined at 600 °C)
Pd/Z	1.0	–	ZrO_2 (calcined at 600 °C)
Pd/ZA-5	1.0	–	5 wt.% ZrO_2/Al_2O_3
Pd/ZA-10	1.0	–	10 wt.% ZrO_2/Al_2O_3
Pd/ZA-15	1.0	–	15 wt.% ZrO_2/Al_2O_3
PdCu/A	1.0	0.3	Al_2O_3 (calcined at 600 °C)
PdCu/Z	1.0	0.3	ZrO_2 (calcined at 600 °C)
PdCu/ZA-5	1.0	0.3	5 wt.% ZrO_2/Al_2O_3
PdCu/ZA-10	1.0	0.3	10 wt.% ZrO_2/Al_2O_3
PdCu/ZA-15	1.0	0.3	15 wt.% ZrO_2/Al_2O_3

fractions of the monoclinic and tetragonal phases of zirconia were calculated with the following equation [30]:

$$X_m = \frac{I_m(\bar{1}\,1\,1) + I_m(1\,1\,1)}{I_m(\bar{1}\,1\,1) + I_m(1\,1\,1) + I_t(1\,0\,1)} \quad (1)$$

where $I_m(\bar{1}\,1\,1)$ and $I_m(1\,1\,1)$ are the line intensities of the $(\bar{1}\,1\,1)$ (at $2\theta = 28.2^\circ$) and $(1\,1\,1)$ (at $2\theta = 31.5^\circ$) peaks for the monoclinic phase (m-ZrO_2) and I_t $(1\,0\,1)$ is the intensity of the $(1\,0\,1)$ (at $2\theta = 30.2^\circ$) peak for the tetragonal phase (t-ZrO_2) of zirconium oxide. The average metal cluster size was determined through XRD line broadening analysis by using Scherrer equation [31]:

$$\tau = \frac{0.9\lambda}{\beta \cos(\theta)} \quad (2)$$

where τ is the crystal size, λ is the wavelength of the Cu Kα radiation, β is the full width half maximum of the respective peak, and θ is the Bragg diffraction angle.

The total acidity of the prepared supports was studied by adsorption of ammonia using a thermobalance (Shimadzu TGA 50). In a typical procedure, the sample was dried in a He flow (30 mL min^{-1}) by heating from room temperature up to 500 °C at a rate of 10 °C min^{-1} to remove adsorbed water and other volatiles. Then, the sample was cooled in a He flow to 70 °C. At that temperature, the catalyst was exposed to an NH_3–He mixture (5 vol.%) at 60 mL min^{-1} flow for the adsorption of the base, until a constant weight was obtained.

SEM/EDX measurements were carried out using a FEI Quanta 200 scanning electron microscope equipped with an energy dispersive X-ray spectroscopy facility (EDX SDD Apollo 40). In order to draw conclusions about the distribution of the components in the samples, Backscattered Electrons (BSE) images were taken.

Temperature-programmed reduction (TPR) experiments were carried out in a conventional flow system built in our laboratory. The reactive gas stream (5% H_2 balanced with Ar) was flowed at 25 mL min^{-1} over 50 mg of sample, and the temperature was raised from room temperature to 800 °C at 10 °C min^{-1}. Hydrogen uptake during the reduction was analyzed on-line by a Shimadzu GC-8A gas chromatograph with a thermal conductivity detector (TCD).

CO adsorption on mono- and bimetallic catalysts was studied by means of FTIR spectroscopy using a Bruker EXINOX 55 equipment. Spectra were recorded at ambient temperature in the 4000–400 cm^{-1} range and the samples were prepared in form of wafers with KBr. The standard sample pretreatment consisted of a reduction in a 20 mL min^{-1} flow of H_2 at 500 °C for 1 h. After that, the samples were cooled in H_2 to room temperature and then flushed with Ar. With the aim of collecting a reference spectrum, a portion of the catalyst was separated, and the rest was exposed to a flow of 10 vol.% CO in He for 30 min at room temperature. Then, the spectrum was collected.

2.4. Catalytic test

The catalytic reduction of nitrates or nitrites was carried out in a 200 mL glass semi-batch reactor equipped with a magnetic stirrer. In a typical run, 100 mL of a solution containing either 100 ppm of NO_3^- (precursor salt: $NaNO_3$) or 100 ppm of NO_2^- (precursor salt: $NaNO_2$) was placed in the reactor. This solution was degassed with N_2. The reaction started when 200 mg of the catalyst, previously reduced under a H_2 flow at 500 °C, was loaded in the reactor. The experiment was carried out at atmospheric pressure, at a temperature of 25 °C and with a H_2 flow of 400 mL min^{-1}. A typical catalytic run was completed after 3 h. To monitor the reaction progress, 1 mL samples were taken periodically. The samples were filtered and then analyzed in an ion chromatograph (Metrohm 790 Personal IC) to determine NO_3^- and NO_2^- concentration. A solution of $NaHCO_3$ 1.0 mM and Na_2CO_3 3.2 mM was used as the mobile phase, the flow rate was set at 7 mL min^{-1}. Ammonium ions were determined by UV–vis spectrophotometry (UV-Vis Thermo Spectronic Helios Gamma), following a modified Berthelot method [32]. The pH value for each sample was also measured.

3. Results and discussion

3.1. Catalyst characterization

Fig. 1(a)–(f) shows the N_2 adsorption–desorption isotherm at −196 °C for each one of the supports used in this work. For all the studied supports, uncalcined ZrO_2 (Fig. 1(a)), Z (Fig. 1(b)) and A (Fig. 1(c)) supports, as well as for the alumina-supported zirconia solids ZA-5, ZA-10 and ZA-15 (all of them calcined at 600 °C), the same type of isotherm was obtained, corresponding to a type IV isotherm according to the IUPAC classification, characteristic of mesoporous solids [33]. The presence of a hysteresis loop in these isotherms is associated with the mechanism of filling and emptying of the pores, which have an ink bottle shape, or with the occurrence of a percolation process due to the effects of interconnection in the pore network. As shown in Fig. 1(d)–(f), the isotherms of the alumina-supported zirconia supports ZA-5, ZA-10 and ZA-15 are identical to the one corresponding to A support (Fig. 1(c)), indicating that the surface characteristics of these supports are quite similar.

Table 1 lists the results of the surface areas of the supports calculated employing the method of Brunauer–Emmett–Teller (S_{BET}). The pore volume and average pore diameter values were obtained using the adsorption branch of the isotherms and are also gathered in Table 1. It can be observed that there is a huge difference between the surface area of the as-prepared and calcined zirconia (Z). Thus, the surface area of the as-prepared zirconia support is 309 m^2 g^{-1}, whereas the Z support has a S_{BET} of 73 m^2 g^{-1} that is more than four times lower. The calcination at 600 °C leads to the collapse of part of the porous structure giving this lower area. The specific surface area of the Z support is quite similar (70 m^2 g^{-1}) to the area obtained by Labaki et al. [34] who prepared ZrO_2 under similar conditions to those used in the present work. From Table 1, it can also be seen that the calcination of ZrO_2 to obtain the Z support caused a reduction in the surface area, but an increase in the average pore diameters. This phenomenon might be derived from a change in the morphology of the support, which could have formed interpores between the particles.

The deposit of ZrO_2 on alumina results in a decrease of the specific surface area of the latter, most probably by pore blocking. This decrease is proportional to the amount of ZrO_2 added. The high surface area of the alumina allows ZrO_2 to be dispersed, creating mixed supports with a significant BET area (184, 179 and 175 m^2 g^{-1} for ZA-5, ZA-10 and ZA-15 samples, respectively (Table 1)).

SEM/EDX analysis was performed to investigate the morphological characteristics of A, Z, ZA-5, ZA-10 and ZA-15 supports (Fig. 2). Fig. 2(a) shows a platy shape surface that corresponds to ZrO_2 according to the EDX analysis. Fig. 2(b) depicts the alumina support presenting its characteristic porous structure. In the three ZA supports it is possible to distinguish separate and individual granules (appearing as bright spots in the micrographs in Fig. 2(c)–(e) due to the use of BSE detection) corresponding to ZrO_2 that has been deposited on Al_2O_3, as is demonstrated by EDX technique. These crystals are distributed homogeneously on the supports indicating a suitable method of preparation and an effective deposit of zirconia on alumina. It can also be seen that ZA supports follow the morphological properties of the mother material.

In order to analyze the structure of pure zirconia and whether this structure is preserved when it is supported on alumina, all the supports were characterized by X-ray diffraction (XRD). According

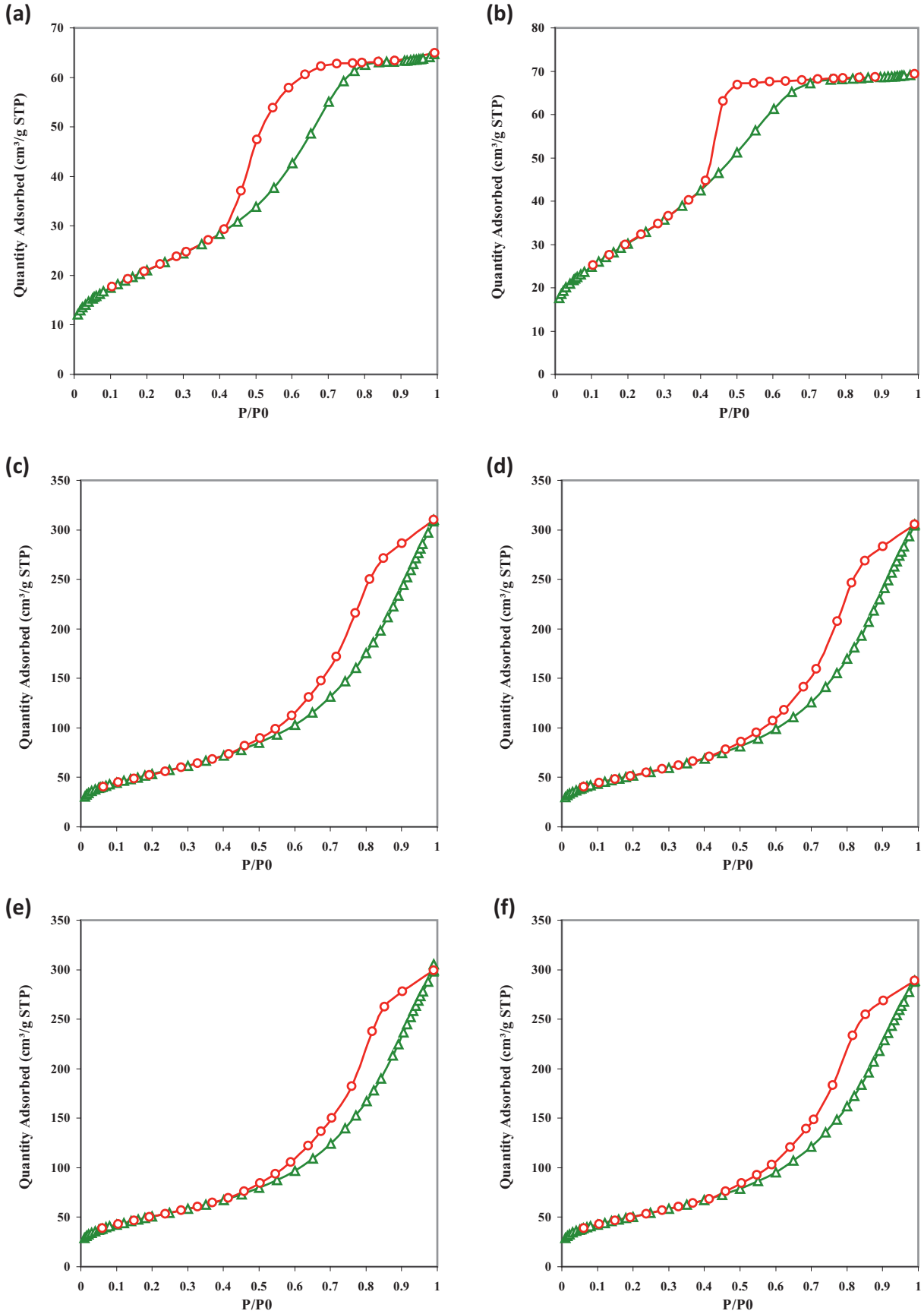

Fig. 1. N_2 adsorption/desorption isotherms at −196 °C for the prepared oxide supports: (a) uncalcined ZrO_2, (b) ZrO_2 calcined at 600 °C (Z), (c) commercial alumina calcined at 600 °C (A), (d) ZA-5, (e) ZA-10, (f) ZA-15.

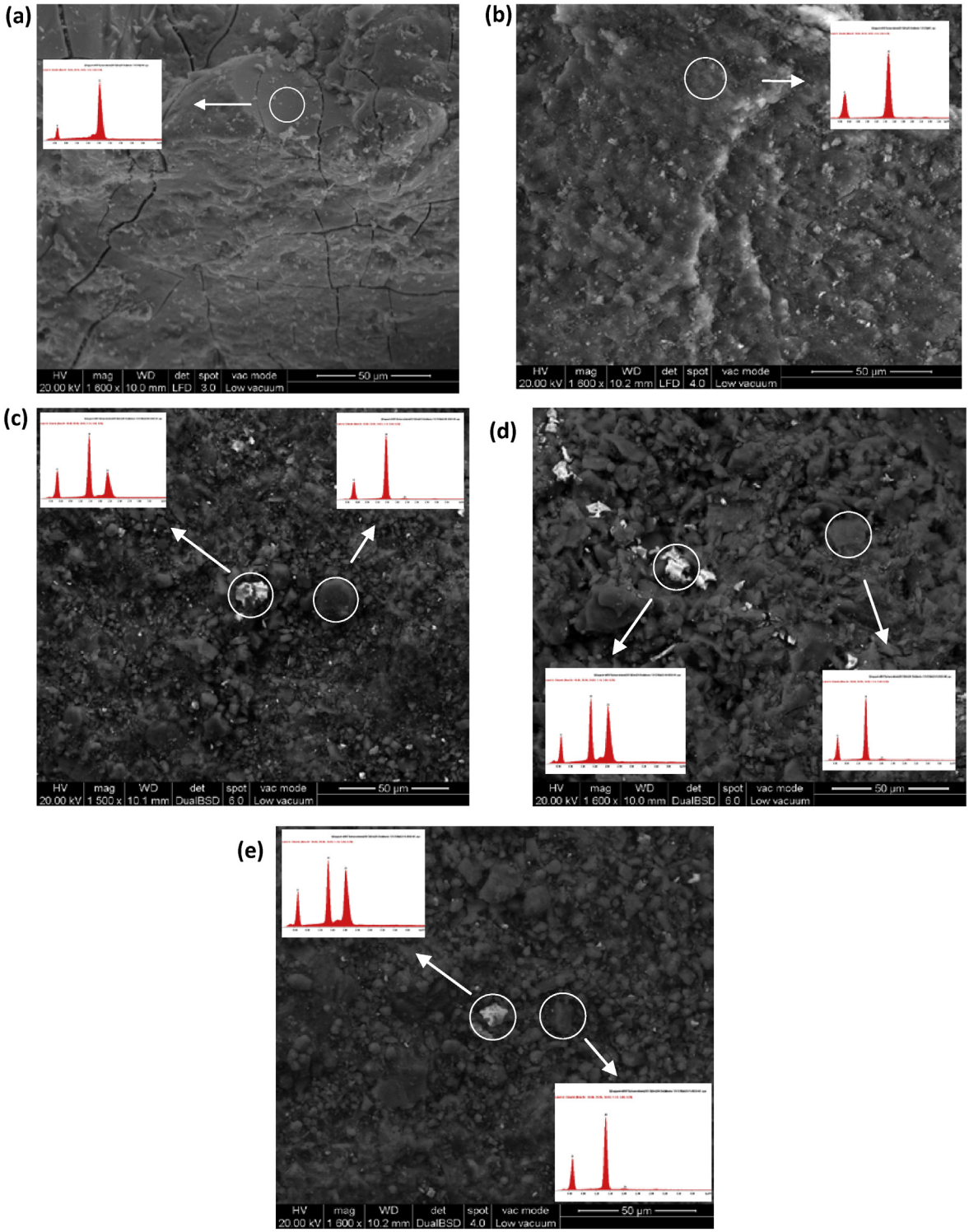

Fig. 2. SEM photographs of Z (a), A (b), ZA-5 (c), ZA-10 (d) and ZA-15 (e) supports.

to literature data, zirconia is amorphous when the calcination temperature is maintained below 300 °C. Crystallization occurs when this material is calcined between 300 °C and 550 °C. In this case, the resulting sample is a mixture of phases corresponding to metastable tetragonal and monoclinic structures [35]. An increase of the calcination temperature leads to the coarsening of the crystallites. The thermodynamically stable monoclinic phase predominates after calcination up to 1200 °C.

Fig. 3 shows the XRD diagram of the Z support. This diagram is similar to that found by Mekhemer et al. [36] who calcined ZrO_2 at 600 °C. In this diagram it is possible to observe the typical diffraction lines of tetragonal metastable structure ($2\theta = 30.5°$, 50.7° and 35.2°) and the diffraction lines characteristic of monoclinic zirconia ($2\theta = 28.2°$, 31.5° and 34.5°). The predominant phase is the metastable tetragonal phase, whose main line is situated at 30.5°, corresponding to the (1 1 1) plane. Using Eq. (1) it can be

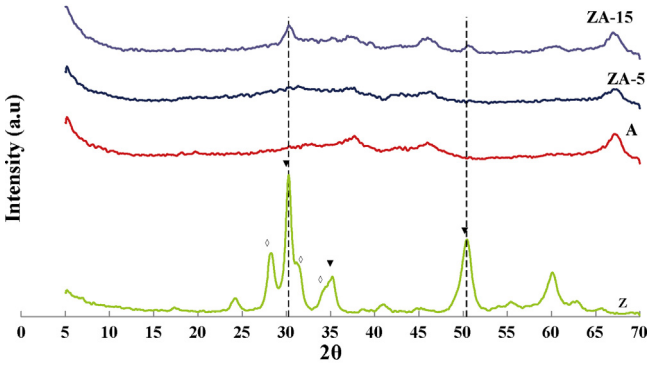

Fig. 3. XRD patterns of Z, A, ZA-5 and ZA-15 supports. (▼) Tetragonal metastable and (◊) monoclinic phases.

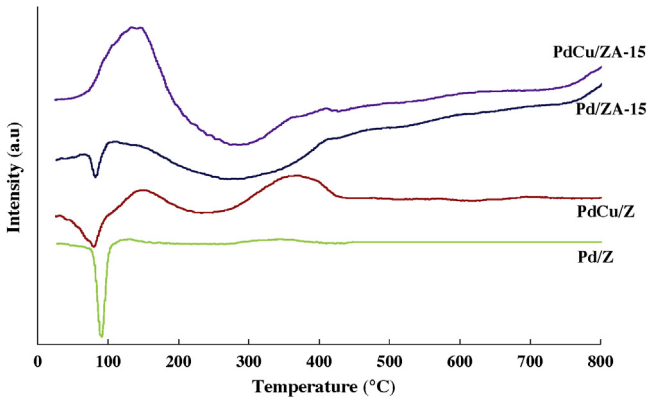

Fig. 4. TPR profiles for Pd/Z, PdCu/Z, Pd/ZA-15 and PdCu/ZA-15 catalysts.

established that the zirconia prepared in this work is a mixture of 43% monoclinic zirconia and 57% metastable tetragonal zirconia. The stabilization of this metastable tetragonal phase is important from the catalytic point of view, especially in what concerns its acidic catalytic properties [37].

During the calcination process, the amorphous $ZrO_2 \cdot nH_2O$ crystallites have different polymorphisms depending on the nature of the host ions. For that reason, it is possible that during the washing process of the hydrogel, the ammonium ions were not completely removed and could probably be oxidized to nitrate ions during calcinations. This leads to the formation of a metastable tetragonal phase [38]. Other authors have found that the presence of oxoanions ($CO_3^{=}$, $SO_4^{=}$, OH^-) increases the stability of the tetragonal phase of zirconia. This may explain the prevailing presence of this phase in our experiments.

For the γ-Al_2O_3 support the structure obtained can be assigned to the hexagonal phase of alumina with a low degree of crystallinity as was proposed by Klimova et al. [26]. The ZA-5 support is almost amorphous, the characteristic peaks are observed neither for the tetragonal nor for the monoclinic phases. When the pattern of ZA-15 is analyzed, it is evident that the crystal structure corresponds to the metastable tetragonal phase, although only the more intense lines at $2\theta = 30.5$ and 50.7° are observed (Fig. 3).

The crystallite sizes of the metastable tetragonal phase on Z and ZA-15 supports estimated from XRD using Eq. (2) have been calculated. The value for pure zirconia (Z) is 23.5 nm, whereas when 15% of ZrO_2 is deposited on alumina this value decreases to 17.6 nm. This result, which can be attributed to the good dispersion achieved, is consistent with those obtained from the morphological studies of the supports.

The results of the acidity measurements evaluated by NH_3-adsorption thermogravimetry are presented in Table 1. From their analysis, it appears that the amount of adsorbed ammonia (expressed as μmol NH_3 m^{-2}) increases with a higher percentage of zirconia in the mixed ZrO_2–Al_2O_3 supports. Thus, the support that showed the highest NH_3-adsorption, ZA-15 with a value of 3.40 μmol NH_3 m^{-2}, is the same one in which the presence of the metastable tetragonal zirconia phase was detected by XRD.

Fig. 4 shows the temperature-programmed reduction (TPR) profiles for the Pd/Z, Pd/ZA-15, PdCu/Z and PdCu/ZA-15 catalysts. The diagrams of Pd/Z, Pd/ZA-15 and PdCu/Z show the presence of a negative peak centered around 85 °C. This peak was studied extensively in the literature for Pd-based catalysts and is indicative of a release of H_2, attributed to the decomposition of β-hydride palladium (H_xPd) formed at room temperature [39–41]. In the case of the TPR profile of the Pd/ZA-15 catalyst, the intensity of the negative peak at 85 °C is strongly reduced, indicating a greater interaction of Pd with the modified support, thus inhibiting the reduction of PdO at low temperatures. Pd/ZA-15 catalyst also present a small and broad peak between 100 and 200 °C in their TPR diagrams, assigned to the reduction of Pd (PdO to Pd°) in accordance with the literature [8].

For the bimetallic PdCu/Z and PdCu/ZA-15 catalysts the TPR profiles are quite different. For the first system, it is possible to distinguish three different peaks: the first peak, around 85 °C that, as already mentioned, corresponds to the decomposition of Pd β-hydride. In relation to the second peak, which is centered around 130 °C, in the literature there are different opinions about which species could be responsible for its existence: some authors assigned it to the reduction of PdO to Pd^0, while other authors assigned it to the reduction of different PdCu species, especially when catalysts are prepared by a catalytic reduction procedure [42,43]. The third peak, which extends between 300 and 400 °C, corresponds to the reduction of CuO to Cu^0 [44]. For the PdCu/ZA-15 catalyst, the negative peak is not observed. This catalyst also shows a broad reduction peak between 60 and 200 °C that can be assigned to the reduction of copper oxides promoted by the presence of the noble metal. As was published by Mendez et al. [41] when studying the reduction of a PdCu/γ-Al_2O_3 catalyst, the absence of the negative peak could be due to the presence of a wide positive peak (between 60 and 150 °C) masking any signal corresponding to the evolution of hydrogen from the decomposition of the hydride phase. These authors stated that it was also possible that the presence of copper within the palladium crystals could inhibit the formation of palladium hydride.

To verify the interaction between palladium and copper species, a series of experiments of CO adsorption followed by FTIR analysis were conducted on Pd/ZA-15 and PdCu/ZA-15 catalysts. The spectra of CO adsorbed on these samples are shown in Fig. 5, for the range between 2250 and 1850 cm^{-1}. Samples without CO adsorbed were taken as reference (Fig. 5, spectra a and c). The band with the maximum around 2060 cm^{-1} (Fig. 5, spectra b and d) is assigned to the presence of CO linearly adsorbed on Pd(0) sites, indicating that the Pd is fully reduced in both catalysts. None of the two samples showed the presence of the band corresponding to bridged CO bonded to Pd (Pd—CO—Pd) at 2020–1800 cm^{-1} [32], which indicates the high dispersion of Pd in both catalysts analyzed. The presence of Cu leads to a decrease in the intensity of linear CO adsorption signal, which is assigned to a decrease of the ability of Pd to adsorb CO caused by Cu.

3.2. Catalytic activity and influence of the copper content

Pd/γ-Al_2O_3, PdCu0.5/γ-Al_2O_3 and PdCu1.0/γ-Al_2O_3 catalysts were evaluated in the catalytic reduction of NO_3^-. The results are depicted in Fig. 6, which represents the NO_3^- concentration decay as a function of time. As has already been mentioned extensively

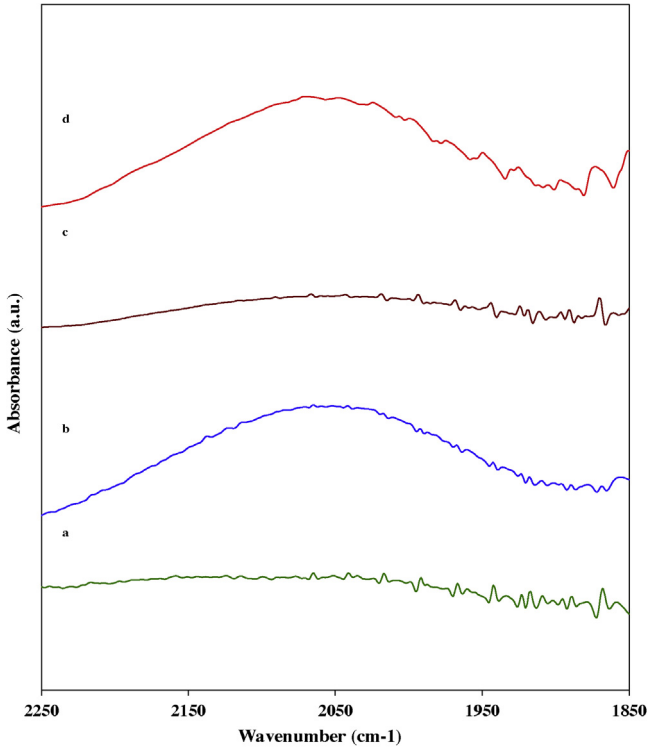

Fig. 5. FTIR spectra of reduced catalysts: (a) Pd/ZA-15, (b) Pd/ZA-15 with CO adsorbed, (c) PdCu/ZA-15, (d) PdCu/ZA-15 with CO adsorbed.

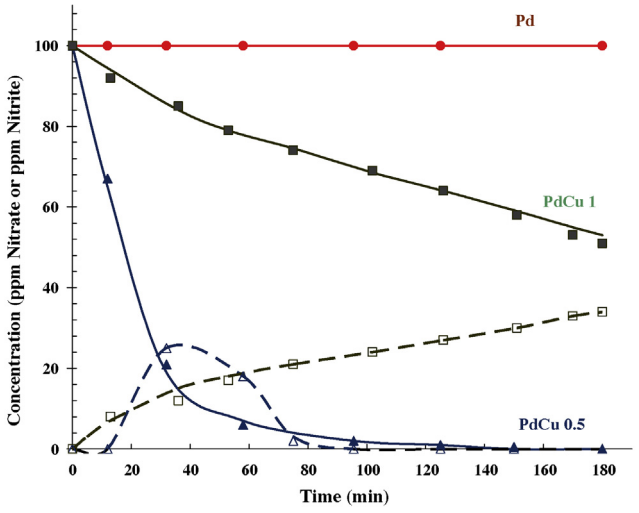

Fig. 6. Nitrate decay (solid lines and symbols) and nitrite formation (dotted lines and open symbols) for γ-Al_2O_3-supported Pd y PdCu catalysts: (●) monometallic Pd/γ-Al_2O_3 catalyst, (▲,△) PdCu0.5/γ-Al_2O_3 catalyst and (■,□) PdCu1.0/γ-Al_2O_3 catalyst.

in the literature [3,44], the Pd/γ-Al_2O_3 catalyst is not active in the reduction of NO_3^-. The bimetallic systems, on the other hand, are active in the reduction of NO_3^- and their reducing capability is clearly dependent on the copper content. Similar to previously published results for PtSn catalysts [5], the highest activity is achieved with the lowest promoter content (PdCu0.5/γ-Al_2O_3 catalyst). For the catalyst with the highest content of copper NO_2^- formation was detected during the course of the reaction, whereas for the PdCu0.5/γ-Al_2O_3 catalyst, although NO_2^- was also generated in the first part of the reaction, it starts to disappear after 40 min, showing the intermediate character of this ion. As regards the generation of NH_4^+ ion, its concentration was determined at the end of the

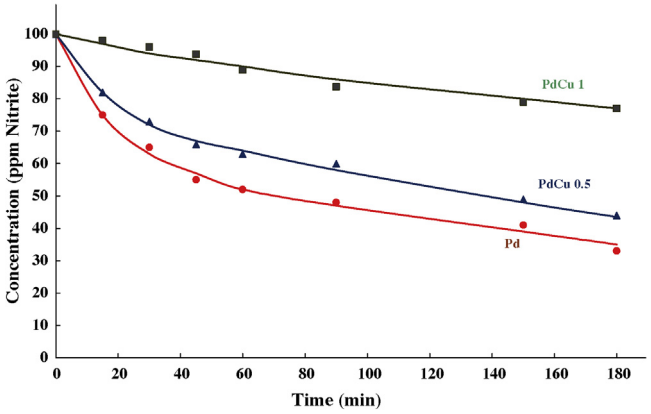

Fig. 7. Nitrite concentration (ppm) in water *vs.* time (min) over Pd/γ-Al_2O_3 (●), PdCu0.5/γ-Al_2O_3 (▲) and PdCu1.0/γ-Al_2O_3 (■) catalysts.

hydrogenation reaction for both bimetallic catalysts, obtaining values of 3 ppm and 7 ppm for PdCu1/γ-Al_2O_3 and PdCu0.5/γ-Al_2O_3, respectively.

The three gamma alumina-supported catalysts, both the monometallic and the bimetallics were active in the removal of NO_2^- (Fig. 7), the monometallic being the most active. Contrary to what happens in the reduction of nitrate, nitrite reduction proceeds rapidly over the monometallic catalyst, in agreement with what is reported in the literature [9].

From the results found in this section, it can be concluded that the bimetallic PdCu0.5/γ-Al_2O_3 catalyst is better than the PdCu1/γ-Al_2O_3 one in terms of activity and, therefore, a Pd/Cu = 0.5 ratio will be used for the rest of the tests performed in this work.

3.3. Catalytic activity and influence of the support

To analyze the influence of the support, the conversion of NO_3^- was examined using both monometallic Pd catalysts and bimetallic PdCu0.5 catalysts supported on all the prepared supports (A, Z, ZA-5, ZA-10 and ZA-15).

Table 3 details the conversion values after 180 min of reaction for the reduction of NO_3^- and NO_2^- anions using monometallic Pd/A, Pd/Z, Pd/ZA-5, Pd/ZA-10 and Pd/ZA-15 catalysts. These conversion values (*X*%) were calculated using the following equation:

$$X\% = \frac{C_i - C_f}{C_i} \times 100 \quad (3)$$

where C_i is the initial concentration of either NO_3^- or NO_2^-, and C_f is the final concentration of the same ion after 180 min of reaction.

All the monometallic catalysts supported on ZrO_2 and ZrO_2-modified Al_2O_3 (Pd/Z, Pd/ZA-5, Pd/ZA-10 and Pd/ZA-15) were active in the reduction of NO_3^-. In order to exclude any influence of the support on the activity of the catalysts toward the reduction of NO_3^-, a blank test for each of the supports in the absence of the metallic phase was carried out. The results indicated that the supports were inert for the NO_3^- reduction. It is well known that when using inert supports such as SiO_2 or Al_2O_3, NO_3^- ion cannot be

Table 3
Nitrate and nitrite conversions (*X*%) determined after 180 min reaction over monometallic catalysts.

Catalyst	*X*(%) NO_3^-	*X*(%) NO_2^-
Pd/A	0	13
Pd/Z	28	33
Pd/ZA-5	17	21
Pd/ZA-10	12	18.5
Pd/ZA-15	8	17

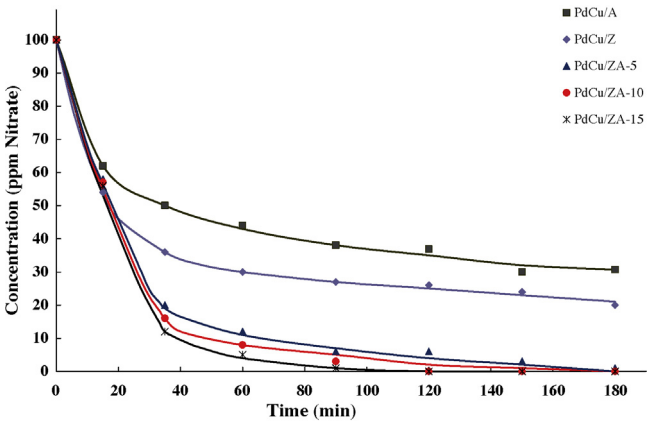

Fig. 8. Nitrate concentration (ppm) in water *vs.* time (min) for nitrate reduction over PdCu catalysts supported on A, Z, ZA-5, ZA-10 and ZA-15. Temperature 25 °C, 400 mL min^{-1} H_2 flow, 200 mg of catalyst.

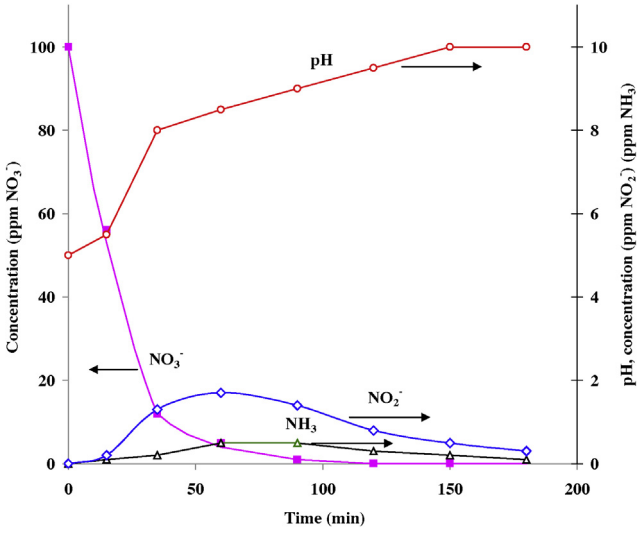

Fig. 9. Nitrate (ppm) consumption, nitrite (ppm) and ammonia (ppm) production and pH variation *vs.* time (min) on PdCu/ZA-15 catalyst. Reaction conditions: Temperature 25 °C, 400 mL min^{-1} H_2 flow, 200 mg of catalyst.

reduced only by the noble metal without a promoter in the denitrification process [11]. Consequently, since the support itself is not active, there must be some interaction between Pd and the ZrO_2-containing supports such that the resulting systems are active in the hydrogenation of NO_3^-. The influence on the catalytic behavior is specifically attributed to ZrO_2 and not to Al_2O_3 since, as has been seen, the monometallic Pd/A catalyst was completely inactive toward the reduction of NO_3^- ion. In the literature there are several references accounting for nitrate reduction using monometallic catalysts in which the support has a promoter effect, such as CeO_2 and TiO_2 [10,17,45]. The reaction mechanism may involve the NO_3^- ion adsorption on the Lewis acid sites (oxygen vacancies) of the tetragonal ZrO_2 through electrostatic interactions. This crystalline phase, as previously explained, represents approximately 60% of the Z support and is the only phase observed in the case of ZA-15 modified support.

The results of the removal of NO_2^- using monometallic Pd catalysts are also reported in Table 3. Like previously obtained results for Pt catalysts supported on γ-Al_2O_3 or SiO_2 [5], and results widely reported in the literature [21,46], all the tested monometallic catalysts were active in the removal of NO_2^-. After 180 min of reaction, the Pd/Z catalyst was the one that reached the highest conversion ($X\%$ = 33), Pd/ZA-5, Pd/ZA-10 and Pd/ZA-15 catalysts showed similar activity (*ca.* $X\%$ = 20) and the Pd/A catalyst was not only the less active but also the less selective to N_2, since at the end of the reaction a concentration of NH_4^+ of 3 ppm was detected.

Then, the hydrogenation of NO_3^- using bimetallic PdCu catalysts was performed and the results are gathered in Fig. 8. The catalytic systems supported on pure ZrO_2 or Al_2O_3 (PdCu/Z and PdCu/A catalysts) were not very promising in terms of activity. The catalytic activity of the PdCu/Z system was slightly higher than that of the PdCu/A catalyst. For the latter, not only a low conversion of NO_3^- was found but also there was a continuous increase in the generation of NO_2^- during the course of the reaction, as well as in the generation of NH_4^+, whose concentration reached a value of 5 ppm at the end of the reaction. The behavior is somewhat different to that obtained with the analog catalyst supported on γ-Al_2O_3, probably due to changes in the support surface.

The results of NO_3^- conversion as a function of time for PdCu/ZA-5, PdCu/ZA-10 and PdCu/ZA-15 catalysts are also shown in Fig. 8. During the first 35 min of reaction, the NO_3^- concentration dropped quickly and, as the reaction progressed, the speed of NO_3^- concentration decrease slowed down. As postulated by several authors [47,48] the increase in pH reduces the rate of conversion of NO_3^-. It is considered that the presence of OH^- ions blocks the access of the NO_3^- ions to the active sites of the catalyst [13].

After 180 min of reaction, the NO_3^- concentration was very low (close to zero) for the three catalysts. Comparing these results with those obtained for the PdCu/A catalyst, it is evident that although the addition of ZrO_2 onto Al_2O_3 did not practically change the textural properties of the alumina as detailed above, it favored a marked improvement in the catalytic performance of the systems toward the conversion of NO_3^-. The high surface area of the ZrO_2–Al_2O_3 mixed supports most likely generates a high dispersion of Pd, facilitating its interaction with copper. This is in agreement with the above-mentioned results found by FTIR, in which the band corresponding to bridged CO bonded to Pd (Pd-CO-Pd) in the region 2020–1800 cm^{-1} was not detected. Also, it goes in the same direction as the modification of the TPR profile of the PdCu/ZA-15 catalyst compared to that of PdCu/Z in what concerns to the negative peak at low temperature. Several authors have attributed the decrease in the negative peak of the TPR profile of PdCu catalysts to the decrease of Pd–Pd pairs upon the addition of Cu [49] and to the fact that part of the Pd is combined with Cu to form bimetallic Pd-Cu ensembles. PdCu catalysts supported on ZrO_2–Al_2O_3 followed a similar pattern to what was found by Strukul et al. [9] using ZrO_2 microspheres as catalytic support for the nitrate removal reaction.

The modification of Al_2O_3 by the addition of ZrO_2 not only improved the activity but also the selectivity to N_2 of the PdCu catalysts. A selectivity analysis was performed on the catalyst that presented the best performance, PdCu/ZA-15, and is shown in Fig. 9. This figure makes it clear that NO_2^- is a reaction intermediate, reaching a maximum concentration of approximately 1.7 ppm and almost disappearing after 180 min. Concerning the ammonia produced during the reaction, although it is dissolved in the aqueous medium, is also carried by the high flow of H_2 used as reagent. The highest concentration of NH_3 detected in the course of the reaction was 0.5 ppm, which is within the acceptable limits for this compound. Regarding the pH variation during the reaction, a rapid and substantial increase from the beginning of the reaction until practically all of the NO_3^- has been consumed was observed. From this point on, a further increase in pH was observed although the intermediate NO_2^- had also been consumed. This fact can be explained by the aforementioned loss of NH_3, which increases the concentration of OH^- in the solution.

For PdCu catalysts it is generally accepted that the reduction of NO_3^- is a reaction that proceeds in steps: initially, the NO_3^- is

reduced to NO_2^- by copper and then a reduction of NO_2^- primarily on Pd sites follows. Cu requires Pd to get stabilized in a partially reduced state by "spillover" of hydrogen [50]. In order to obtain this effective stabilization of Cu, an intimate contact between Pd and Cu is required. When analyzing the TPR profile of the PdCu/ZA-15 catalyst used in this work, for example, the presence of a significant hydrogen consumption peak assigned to the joint reduction of Pd and Cu can be observed, thus indicating that both species are actually in intimate contact.

4. Conclusions

A series of monometallic Pd catalysts and Cu-promoted Pd-based catalysts were prepared using alumina and ZrO_2-modified alumina as supports. All of them were tested in the NO_3^- reduction reaction.

The three ZrO_2-modified Al_2O_3 supports (ZA-5, ZA-10 and ZA-15) showed a BET area slightly lower than that of the alumina, but well above the area of the original zirconia. XRD studies of these supports shown that the predominant phase of the zirconia is the metastable tetragonal phase (57%), an important characteristic from the catalytic point of view. In the SEM images of the three ZA supports individual granules of ZrO_2 deposited on Al_2O_3 were distinguished. These crystals are distributed homogeneously on the supports indicating a suitable method of preparation and an effective deposition of zirconia on alumina.

In the TPR pattern of the PdCu/ZA-15 catalyst, which had a very good performance in reducing the nitrate ions, the negative peak corresponding to the decomposition of the Pdβ-hydride was either not observed or its intensity was greatly diminished, indicating that Pd is well dispersed on the support. Also, the presence of a peak at around 130 °C, assigned to the reduction of different Pd-Cu species, is indicative of the strong interaction between the two metals.

From the series of monometallic Pd catalysts studied, only the one supported on alumina was inactive in the reduction of NO_3^-, in agreement with the literature. The other monometallic catalysts were active, showing the ability of the support to activate NO_3^- due to its redox properties.

Cu addition to Pd/A substantially enhanced the activity toward NO_3^- conversion, although both NO_2^- and NH_4^+ during the course of the reaction are generated. The modification of Al_2O_3 by the addition of ZrO_2 not only improved the activity but also the selectivity to N_2 of the PdCu catalysts.

Acknowledgements

The authors are grateful to the Consejo Nacional de Investigaciones Científicas y Técnicas (CONICET) (Argentina) (PIP 0185) and the Universidad Nacional de La Plata (UNLP I152 and X633) (Argentina).

References

[1] EPA, Basic Information about Nitrate in Drinking Water, 2012 http://water.epa.gov/drink/contaminants/basicinformation/nitrate.cfm
[2] E.R. Jaffe, Clin. Haematol. 10 (1981) 99–122.
[3] N. Barrabés, J. Sá, Appl. Catal. B 104 (2011) 1–5.
[4] G. Mendow, F.A. Marchesini, E.E. Miró, C.A. Querini, Ind. Eng. Chem. Res. 50 (2011) 1911–1920.
[5] M.A. Jaworski, V. Vetere, H.P. Bideberripe, G.J. Siri, M.L. Casella, Appl. Catal. A 453 (2013) 227–234.
[6] J. Sá, D. Gasparovicova, K. Hayek, E. Halwax, J.A. Anderson, H. Vinek, Catal. Lett. 105 (2005) 209–217.
[7] A.E. Palomares, C. Franch, A. Corma, Catal. Today 149 (2010) 348–351.
[8] U. Prusse, K.D. Vorlop, J. Mol. Catal. A: Chem. 173 (2001) 313–328.
[9] G. Strukul, R. Gavagnin, F. Pinna, E. Modaferri, S. Perathoner, G. Centi, M. Marella, M. Tomaselli, Catal. Today 55 (2000) 139–149.
[10] J. Sá, T. Berger, K. Fottinger, A. Riss, J.A. Anderson, H. Vinek, J. Catal. 234 (2005) 282–291.
[11] O.S.G.P. Soares, J.J.M. Órfão, M.F.R. Pereira, Catal. Lett. 126 (2008) 253–260.
[12] L. Lemaignen, C. Tong, V. Begon, R. Burch, D. Chadwick, Catal. Today 75 (2002) 43–48.
[13] M. D'Arino, F. Pinna, G. Strukul, Appl. Catal. B 53 (2004) 161–168.
[14] F. Epron, F. Gauthard, J. Barbier, J. Catal. 206 (2002) 363–367.
[15] A. Garron, K. Lazar, F. Epron, Appl. Catal. B 59 (2005) 57–69.
[16] N. Barrabés, A. Frare, K. Föttinger, A. Urakawa, J. Llorca, G. Rupprechter, D. Tichit, Appl. Clay Sci. 69 (2012) 1–10.
[17] O.S.G.P. Soares, J.J.M. Órfão, M.F.R. Pereira, Desalination 279 (2011) 367–374.
[18] O.S.G.P. Soares, J.J.M. Órfão, M.F.R. Pereira, Appl. Catal. B 102 (2011) 424–432.
[19] K. Vorlop, T. Tacke, Chem. Ing. Tech. 61 (1989) 836–845.
[20] N. Barrabes, J. Just, A. Dafinov, F. Medina, J.L.G. Fierro, J.E. Sueiras, P. Salagre, Y. Cesteros, Appl. Catal. B 62 (2006) 77–85.
[21] K. Wada, T. Hirata, S. Hosokawa, S. Iwamoto, M. Inoue, Catal. Today 185 (2012) 81–87.
[22] K. Tanabe, Mater. Chem. Phys. 13 (1985) 347–364.
[23] Y. Amenomiya, Appl. Catal. 30 (1987) 57–68.
[24] L. Escandón, S. Ordóñez, A. Vega, F. Díez, Chemosphere 58 (2005) 9–17.
[25] H. Tidahy, S. Siffert, F. Wyrwalski, J. Lamonier, A. Aboukaïs, Catal. Today 119 (2007) 317–320.
[26] T. Klimova, M.L. Rojas, P. Castillo, R. Cuevas, J. Ramírez, Microporous Mesoporous Mater. 20 (1998) 293–306.
[27] A. Kytökivi, E.-L. Lakomaa, A. Root, H. Österholm, J.-P. Jacobs, H.H. Brongersma, Langmuir 13 (1997) 2717–2725.
[28] S. Korhonen, S. Airaksinen, M. Bañares, A. Krause, Appl. Catal. A 333 (2007) 30–41.
[29] S. Damyanova, P. Grange, B. Delmon, J. Catal. 168 (1997) 421–430.
[30] H. Toraya, M. Yoshimura, S. Somiya, Commun. Am. Ceram. Soc. (1984) 119–121.
[31] A.L. Patterson, Phys. Rev. 56 (1939) 978–982.
[32] F.A. Marchesini, L.B. Gutierrez, C.A. Querini, E.E. Miró, Chem. Eng. J. 159 (2010) 203–211.
[33] K.S.W. Sing, D.H. Everett, R.A.W. Haul, L. Moscou, R.A. Pierotti, J. Rouquerol, T. Siemieniewska, Pure Appl. Chem. 57 (1985) 603–619.
[34] M. Labaki, S. Siffert, J.-F. Lamonier, E.A. Zhilinskaya, Antoine Aboukaïs, Appl. Catal. B 43 (2003) 261.
[35] Q. Chang, J.-E. Zhou, Y. Wang, G. Meng, Adv. Powder Technol. 20 (2009) 371–374.
[36] G.A.H. Mekhemer, Colloids Surf. A 274 (2006) 211–218.
[37] V.G. Deshmane, Y.G. Adewuyi, Microporous Mesoporous Mater. 148 (2012) 88–100.
[38] A.F. Wells, Structural Inorganic Chemistry, 5th ed., Oxford University Press, New York, 1986.
[39] V.H. Sandoval, C.E. Gigola, Appl. Catal. A 148 (1996) 81–96.
[40] M.L. Cuberiro, J.L.G. Fierro, Appl. Catal. A 168 (1998) 307–322.
[41] C.M. Mendez, H. Olivero, D.E. Damiani, M.A. Volpe, Appl. Catal. B 84 (2008) 156–161.
[42] J. Sá, H. Vinek, Appl. Catal. B 57 (2005) 247–256.
[43] H-d. Zhuang, S.-f. Bai, X.-m. Liu, Z.-f. Yam, J. Fuel Chem. Technol. 38 (2010) 462–467.
[44] D. Găsparovičová, M. Králik, M. Hronec, Z. Vallůsová, H. Vinek, B. Corain, J. Mol. Catal. A: Chem. 264 (2007) 93–102.
[45] W. Sun, Q. Li, S. Gao, J.K. Shang, Appl. Catal. B 125 (2012) 1–9.
[46] F. Deganello, L.F. Liotta, A. Macaluso, A.M. Venezia, G. Deganello, Appl. Catal. B 24 (2000) 265–273.
[47] Y. Wang, J. Qu, H. Liu, J. Mol. Catal. A: Chem. 272 (2007) 31–37.
[48] S. Bae, J. Jung, W. Lee, Chem. Eng. J. 232 (2013) 327–337.
[49] Z. Xu, L. Chen, Y. Shao, D. Yin, S. Zheng, Ind. Eng. Chem. Res. 48 (2009) 8356–8363.
[50] O.M. Ilinich, E.N. Gribov, P.A. Simonov, Catal. Today 82 (2003) 49–56.